U. S. Geological Survey.

REPORTS-OPEN FILE SERIES, no. 77-94: 1977.

UNITED STATES DEPARTMENT OF THE INTERIOR

GEOLOGICAL SURVEY.

Mapping the lateral boundaries of a cooling basaltic lava lake, Kilauea Iki, Hawaii

By

Vincent J. Flanigan and Charles J. Zablocki, 1928-

Open-File Report 77-94

1977

This report is preliminary and has not been edited or reviewed for conformity with U.S. Geological Survey standards

Mapping the lateral boundaries of a cooling basaltic lava lake, Kilauea Iki, Hawaii

By

Vincent J. Flanigan and Charles J. Zablocki

Introduction

Two types of electromagnetic (EM) profiling techniques were used to delineate the surface projection of the edges of the still-molten basaltic lava lens that exists in Kilauea Iki Crater, Hawaii. These studies were made as part of an intensive geophysical program aimed at defining the overall configuration of the liquid core and the attendant hydrothermal fluids. The results of the profiling studies were presented orally at the Annual Fall Meeting of the American Geophysical Union held in San Francisco, Calif., December 6, 1976. This report summarizes in more detail the techniques, results, and some conclusions related to the EM profiling studies. The complete results of an intensive VLF study made by L. A. Anderson (U.S. Geol. Survey, oral communication, 1976) will be presented in a separate report. Only a few of these results are discussed here.

Turam Study

One EM profiling technique used in this study was the turam method (see Keller and Frischknecht, 1966, pp. 396-409). Measurements of the ratio of the magnitude of the vertical magnetic field and the phase differences between the two horizontal, circular-loop receivers were made along 9 traverses that were extended radially from a horizontal, circular-transmitter loop positioned on the central part of the lake surface (fig. 1). The transmitter loop (61 m diameter) was excited at 200, 400, and 800 Hz.

The two receiver coils (0.5 m diameter) were spaced 30.5 m apart and measurements were made at 30.5 m intervals along each traverse.

The field ratios were normalized by dividing by ratios computed from the expression for the primary field in free space. In the absence of conductive material, the normalized ratio is always unity. The normalized field ratios were contoured and rather small differences were noted in the patterns between the three frequencies used. Figure 2 shows the distribution of the normalized field ratios obtained at 400 Hz. It is seen that the normalized ratios are radially asymmetric in that slightly larger amplitude ratios (about 10%) were obtained along the north and south sides of the lake than along the east and west sides. The asymmetry may be caused by differences in the conductivity, thickness, and or depth of the molten basalt in these areas, or may be partly a consequence of the different lateral distances between the transmitter and the molten lava edges.

The dotted line on the contour map (fig. 2) outlines the interpreted edge of the molten lava. The interpretation was based on physical scale model studies to be discussed in the following section.

The real and imaginary parts of the vertical magnetic field at 400 Hz were computed for each traverse from the measured amplitude ratio and phase differences. The real component computed from measurements along the east traverse is shown in figure 3. The amplitude is in percent from an arbitrary point, chosen at A/R = 2 where A is the distance from the center of the transmitting loop to the center of the detector coil spread and R is the radius of the transmitting loop. A/R is dimensionless and was used to compare directly the field and scale model data. The shaded area outlined on figure 3 shows the spread of all the field curves (real component) from the nine traverses. Plots of the imaginary component obtained from four of the field curves are shown in figure 4. There is considerably more variation between the imaginary component field curves than there is between the real component field curves because the imaginary component is more sensitive to lateral changes of conductivity. Thus, these variations may be reflecting small variances in the conductivity of the melt, different conductivity gradients at the melt edges, and/or differences in the depth to melt.

Scale model studies

Scale model studies were made to determine the relationship between the edge of the melt and the real component of the electromagnetic field. Scale modeling, as applied to electromagnetic methods, is described in detail by Frischknecht (1971). The real component was used because it was more consistent than the imaginary component. The scale factor, transmitting frequency, and conductivity-thickness parameter were chosen such that the induction number of the model was approximately equal to the induction number of the molten lens. Values of the melt conductivity and thickness, estimated from other studies (Smith and others, 1977) were used for determining the field induction number. In the scale model studies, in-phase and quadrature components of the electromagnetic field were measured directly, rather than measuring ratios and phase differences as in the field survey. A schematic drawing of the tank model set-up is shown in figure 5. The scaled transmitting loop was located over the center of a nearly circular conductive disc in air. The detector coil was mounted on a movable trolley, and measurements were made at specific distances from the center of the transmitting loop. Measurements were made at several levels between the center of the transmitting coil and the center of the conductor in order to establish the amplitude of the real response. At an appropriate distance between the coil and conductor, measurements were made using conductive discs of various sizes. The value of the real component of the vertical magnetic field for three sizes of conductors measured is shown in figure 6. The scaling factor in this study was such that curve 1 represents a conductor 720 m in diameter, and curves 2 and 3 represent conductors 640 m and 520 m in diameter respectively. The diameter of the conductor has little effect on the shape of the real response curve at distances from the transmitting loop less than A/R = 3. At larger A/R values, the response curves diverge toward the edge of the respective conductive disc. Numbered tick marks show the location of the edge of the model conductors in relationship to the numbered curves (fig. 6). The distance between the inflection point on each curve, representing the point of steepest gradient, or highest amplitude ratio, and the edge of the conductor varies from about 21 to 31 m. An example of a model curve fitted to a field curve is shown in figure 7. The circled points are the model response values that correspond to a conductor 640 m in diameter. As seen in figure 7, the fit is only approximate and would require further modeling to obtain a better fit. Nevertheless, the edge of the conductor is about 31 m beyond the point of highest amplitude ratio. Using this emperical relationship, the conductor edge of the lava lake was estimated from the data for each profile. The interpreted surface projection of the conductor edge along the nine traverses (fig. 2) is accurate to within ±10 meters if the physical scale model is an accurate representation of the melt. The interpreted edge, interpolated between the traverses, may be less accurate.

At the frequencies used in this study (200, 400, and 800 Hz), the induced currents are mostly concentrated in the melt rather than in the less conductive liquid-phase water zone that overlies and flanks the edges of the melt. At these low frequencies, however, the real component measurements do not allow for discerning any irregular and fine details in the configuration of the melt edge that may exist. In retrospect, a transmitter loop placed outside the melt zone, or a single loop placed around the outer perimeter of the lava lake, may be more effective in delineating the configuration of the melt edge.

VLF (very low frequency) Studies

Previous studies have demonstrated the utility of the VLF method for delineating the surface projection of the conductive edge of the melt in some areas of the lava lake in Kilauea Iki (Zablocki, 1976). Further VLF studies have been made recently by L. A. Anderson (U.S. Geol. Survey, oral communication, 1976). In Anderson's study, the tilt angle and ellipticity of the polarization ellipse of the magnetic field and the complex scalar-surface impedance were measured using VLF transmitter stations NLK (frequency = 18.6 kHz; azimuth = N34°E) and NPM (frequency = 23.4 kHz; azimuth = N53°W) as sources. Measurements were made at 30 m (100 ft.) intervals along parallel and perpendicular traverses spaced approximately 60 m (200 ft.) apart. The azimuths of the traverses approximately coincided with the bearings to the two VLF sources (fig. 2).

Four apparent resistivity profiles obtained along the two traverses shown in figure 2, using NLK and NPM as sources, typify the response obtained in this study (fig. 8). The numbered bars in figures 2 and 8 mark the approximate surface projection of the melt edges. Over the central part of the lake, the apparent resistivities measured at 18.6 kHz generally are lower than those measured at 23.4 kHz. These differences in the resistivity are probably related to the small, but significant, differences in the induction numbers at these two frequencies (12 percent) and the conductivity distribution with depth. The apparent resistivities at these two frequencies are in accord with those computed for some one-dimensional, multi-layered models. It is significant that these one-dimensional models required the presence of both a low resistivity layer above the melt (120 ohm-m) as well as a much lower resistivity for the melt zone(assumed to be 2 ohm-m).

The relatively larger variations in the apparent resistivities at the higher frequency may result partly from shallow, lateral changes in resistivity that are not as responsive at the lower frequency. The increase in apparent resistivity toward the inferred edges of the flat, conductive lens is quite dramatic for the measurements made in the TM (transverse magnetic) mode in contrast to those measurements made in the TE (transverse electric) mode. Such responses are consistent with EM theory; they are due to electric field discontinuities across conductivity boundaries. The high resistivity zone that borders the conductive edge does not continue to the outer edge of the lake, but is separated by a narrow (< 30 m wide) moderately conductive zone that lies about 60 m beyond the conductive lens edge.

These results prompt a conceptual model (fig. 9) that might qualitatively explain the lateral distribution of the observed resistivities. The configuration of the pre-filling crater surface along the north side of the lava lake was taken from a lava-thickness contour map compiled by R. T. Holcomb (U.S. Geol. Survey, written communication, 1976). The depth to the top of the melt zone and the temperature isotherms in the overlying crust were taken from data derived from a hole drilled by the U.S. Geological Survey in early 1975 (DH-75-3 in figure 2). The other features shown in the model are conjectural, some of which might be amenable to testing by analytical studies. The existence of a wet zone above the melt, derived from condensing steam rising from the underlying hot lavas, is inferred from the galvanic and induction soundings reported elsewhere (Zablocki, 1976, Smith and others, 1977) and from in-hole temperature data (Peck, 1974; Zablocki and Tilling, 1976). The extrapolated contours for the 500° C and 100° C isotherms around the edge and below the melt zone are shown as extending farther away from the melt than they do on top. Heat transfer by conduction would be the dominant mechanism in these regions, whereas faster heat transfer by convection would dominate above the meet. The heavy rainfall (200-250 cm/yr) on the lake surface could sustain hydrothermal convection over the melt and at the margins. The pattern of the convection cells, characterized by the conditions for marginal stability, are unknown, but may be of the form shown in the model. Accordingly, the generalized resistivity profile shown above the model in figure 9 could be explained as follows: The low resistivities over the central part of the lake result from both liquid-phase water and the ionically conductive melt. The low resistivities might extend outward 10 to 15 m past the melt zone where the temperature may still be high enough (> 500°C) to render the lavas moderately conductive. In the region where the temperatures are below 500°C, but above boiling, the lavas would have very high resistivities and the overlying waters may exist primarily in a vapor phase. These two conditions could explain the exceptionally high resistivity zone bordering the melt edge. Beyond this zone, the ascending water vapor may be condensed in a narrow zone at a shallow depth owing to a relatively large volume of meteoric water that would be guided inward if the surrounding older lavas have a lower macroscopic permeability (fewer fractures). The condensed steam could contain large concentrations of salts to enhance the low resistivity in this zone. In Hawaiian lava lakes, salts condense as incrustations along the numerous cracks in the cooler parts of the crust (Peck and Minakami, 1968). The sublimates in the upper crust over the central part of the lake may be leached by meteoric waters and condensed steam. The dissolved salts could then migrate laterally along the liquid-water surface to the lake margin where they would mix with the cooler water. Beyond this narrow and moderately conductive zone, the lavas would be partially desaturated with cold groundwater and would result in the high resistivities shown here and which are known to occur in other near-surface Kilauea lavas.

It is important to realize that the gradients of the resistivity anomalies toward the lake margins are fairly steep (15-20 m) and therefore indicate that the tops of the causative zones must lie at correspondingly shallow depths. Notwithstanding the complex development of the lava lake during which 17 eruptive phases were associated with crustal foundering and drainback, the likelihood of small isolated pockets of melt still existing at shallow depths after 17 years of cooling seems remote. It would appear then, that hydrothermal factors, such as those presented here, must strongly be influencing the responses obtained by these VLF measurements.

Conclusions

Further scale model studies might help refine the interpretation of the turam data presented here, but at the low frequencies and transmitter configuration used in this study, it is questionable that such additional efforts would be worthwhile. Further emphasis might better be placed on making a turam survey in which the transmitting loop was placed outside the regions of the melt. In this manner, not only would larger anomalies result from the melt edge, but further information could be gained about the hydrothermal system around the lake margin.

The inferred melt edge deduced from this turam study and the two VLF profiles shown in figure 2 are in agreement to within only ±30 m (in the worst case). The differences must reflect the complex electrical nature of the margins. The much higher frequencies of the VLF method allow for detecting narrower and less conductive features in the lake than does the turam method. The turam method, however, has an interpretive advantage over the VLF method in that the source location and frequencies can be controlled. The use of an additional profiling method such as Slingram would also aid in the intepretation of the complex electrical nature of the lake margin.

References

Frischknecht, F. C., 1971, Electromagnetic scale modelling, in Electromagnetic probing in geophysics: J. R. Wait (ed.) Golem Press, Boulder, Colorado, pp. 265-320.

Keller, G. V., and Frischknceht, F. C., 1966, Electrical methods in geophysical prospecting: Permagon Press, Oxford.

Peck, D. L., 1974, Thermal properties of basaltic magma: results and practical experience from study of Hawaiian lava lakes: in Proceedings of the U.S.-Japan Joint Science Seminar on Volcano Energy (Hilo, Hawaii, Feb. 4-8, 1974).

Peck, D. L., and Minakami, Takishi, 1968, The formation of columnar joints in the upper part of Kilauean lava lakes, Hawaii: Geol. Soc. America Bull., v. 79, p. 1151-1166.

Smith, B. D., Zablocki, C. T., Frischknecht, F. C., and Flanigan, V. J., 1977, The geoelectric structure of Kilauea Iki lava lake, Hawaii: U.S. Geol. Survey Open-File report 77-59, 9 p., 14 fig.

Zablocki, C. J., 1976, Some electrical and magnetic studies of Kilauea Iki lava lake, Hawaii, U.S. Geological Survey Open-File report 76-304.

Zablocki, C. J., and Tilling, R. I., 1976, Field measurements of apparent Curie temperatures in a cooling basaltic lava lake, Kilauea Iki, Hawaii: Geophys. Res. Letters, v. 3, no. 8, pp. 487-490.

Figure Captions

Fig. 1. Plan map of Kilauea Iki lava lake, showing location of turam. Survey nails indicated by x and a number.

Fig. 2. Contour map of Kilauea Iki lava lake, showing the turam amplitude ratio of the vertical electromagnetic field measured between two detector coils 30 m apart from a 400 Hz signal generated by the centrally located transmitting loop shown in figure 1. The dotted line shows the interpretated edge of the conductive melt from model studies. The numbered ticks show the edge of the melt interpretated from the VLF data obtained along two orthogonal traverses.

Fig. 3. Real component of the electromagnetic field, Kilauea Iki lava lake. The ordinate is in percent of field from an arbitrary point. The abscissa is the ratio of A/R where A is the distance from the center of the transmitting loop to the center of the two receiver loops and R is the radius of the transmitting loop. Shaded region shows the range in the field curves obtained along all 9 traverses.

Fig. 4. Imaginary components of the electromagnetic field obtained along 4 traverses. The dashed curve is a typical imaginary model response curve.

Fig. 5. A schematic drawing of the turam modeling set up.

Fig. 6. Model curves of the real component of the vertical magnetic field over conductors of various diameters. Curve 1 represents a conductive body 720 m diameter, curves 2 and 3 represent conductors 640 and 520 m respectively. Heavy tick marks (1, 2, and 3) show location of edge of model conductor in relation to curve.

Fig. 7. Real component of a model curve, (circles) and the real component of the east field traverse. The edge of the conductive model represents a field distance of 320 m from the center of the transmitting loop.

Fig. 8. Apparent resistivity profiles obtained along traverses shown in figure 2. Circled-numbers show locations of conductor edge (data from L. A. Anderson (written communication, 1976).

Fig. 9. Conceptual model of the north edge of the lava lake showing the possible configuration of the melt lens, the hydrothermal system, and temperature distribution within the lake that might account for the generalized resistivity profile shown on top.

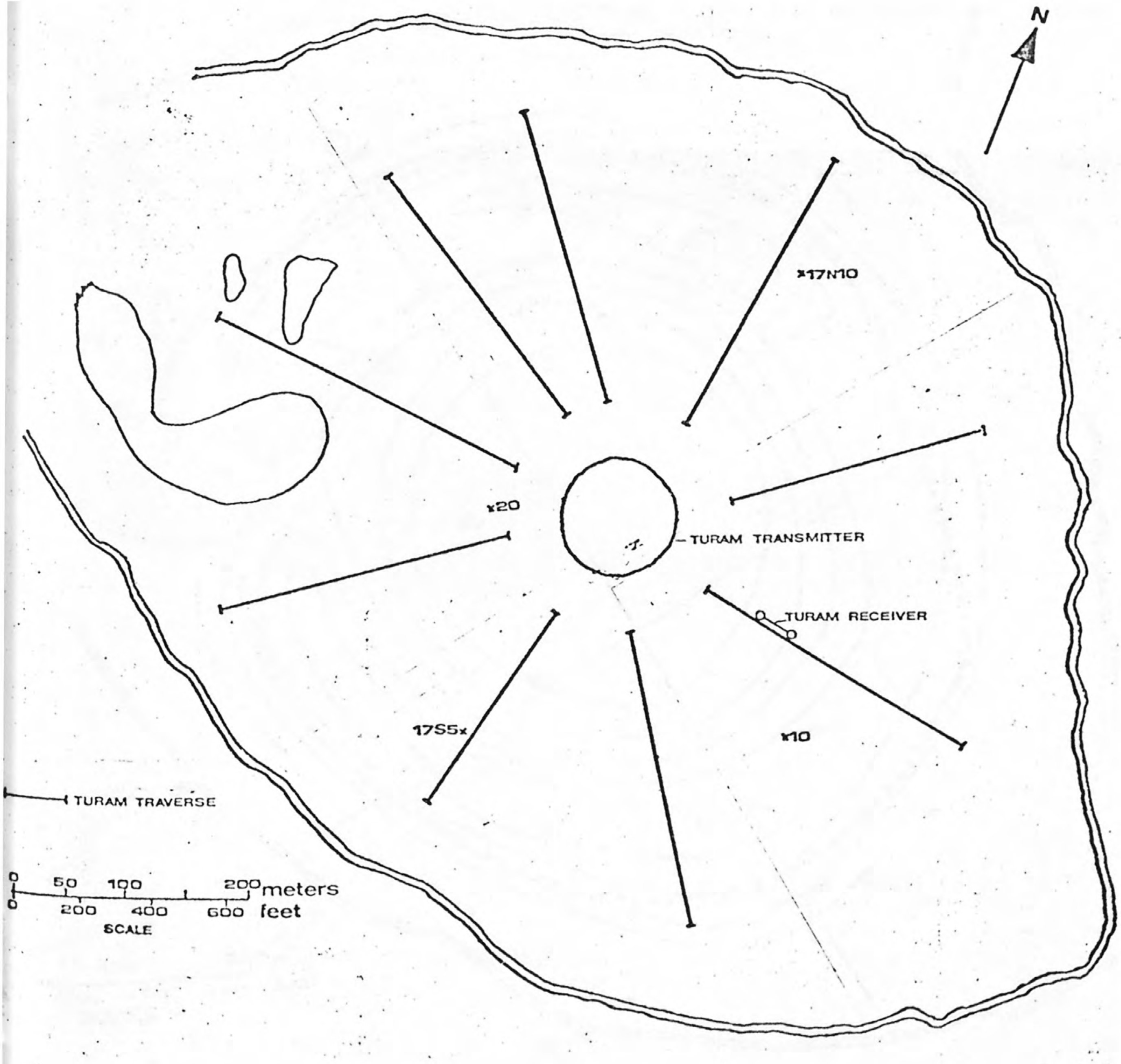

Figure 1. GEOPHYSICAL SURVEY OF KILAUEA IKI, HAWAII

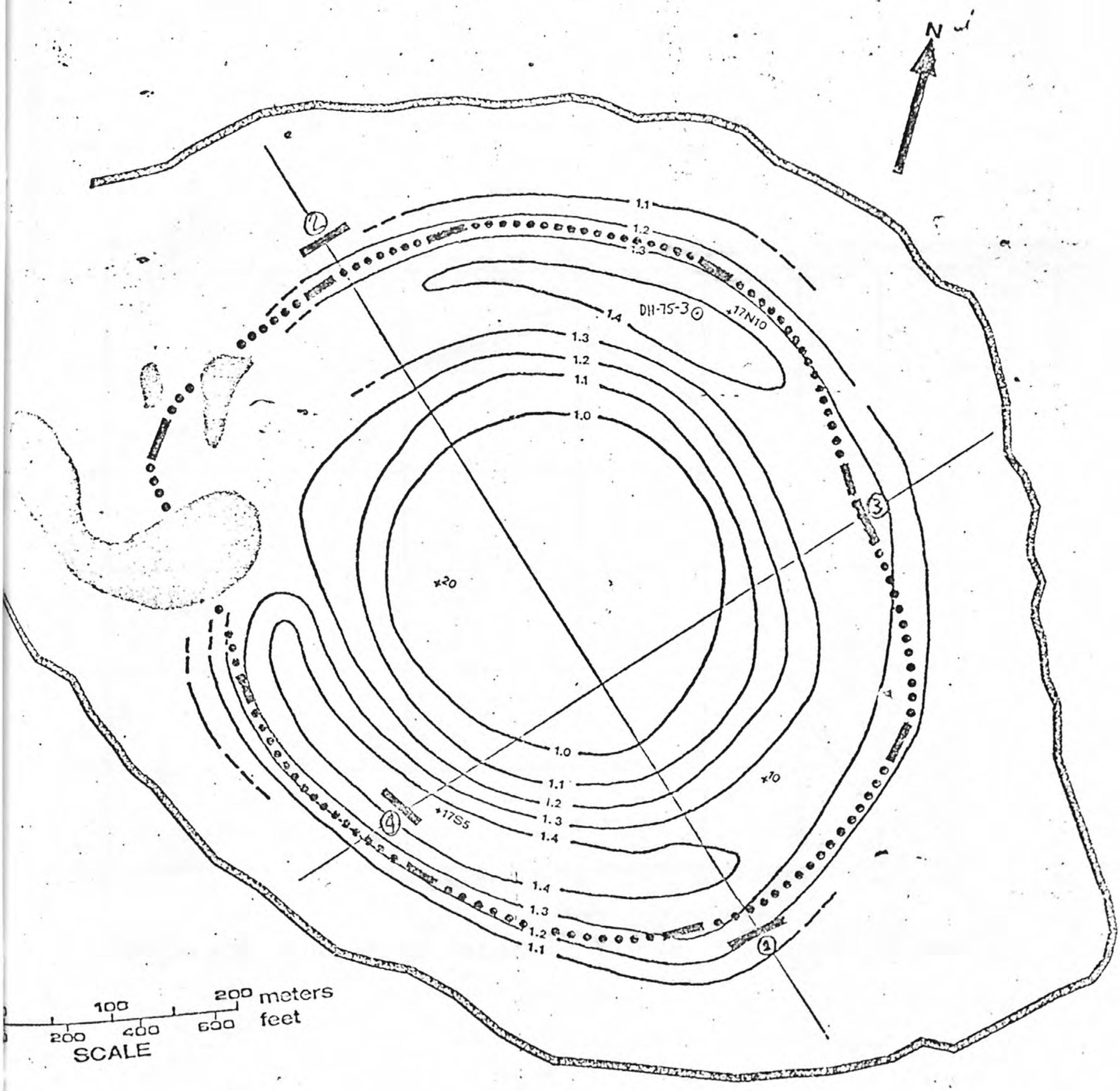

Figure 2. Turam amplitude ratios, Kilauea Iki, Hawaii

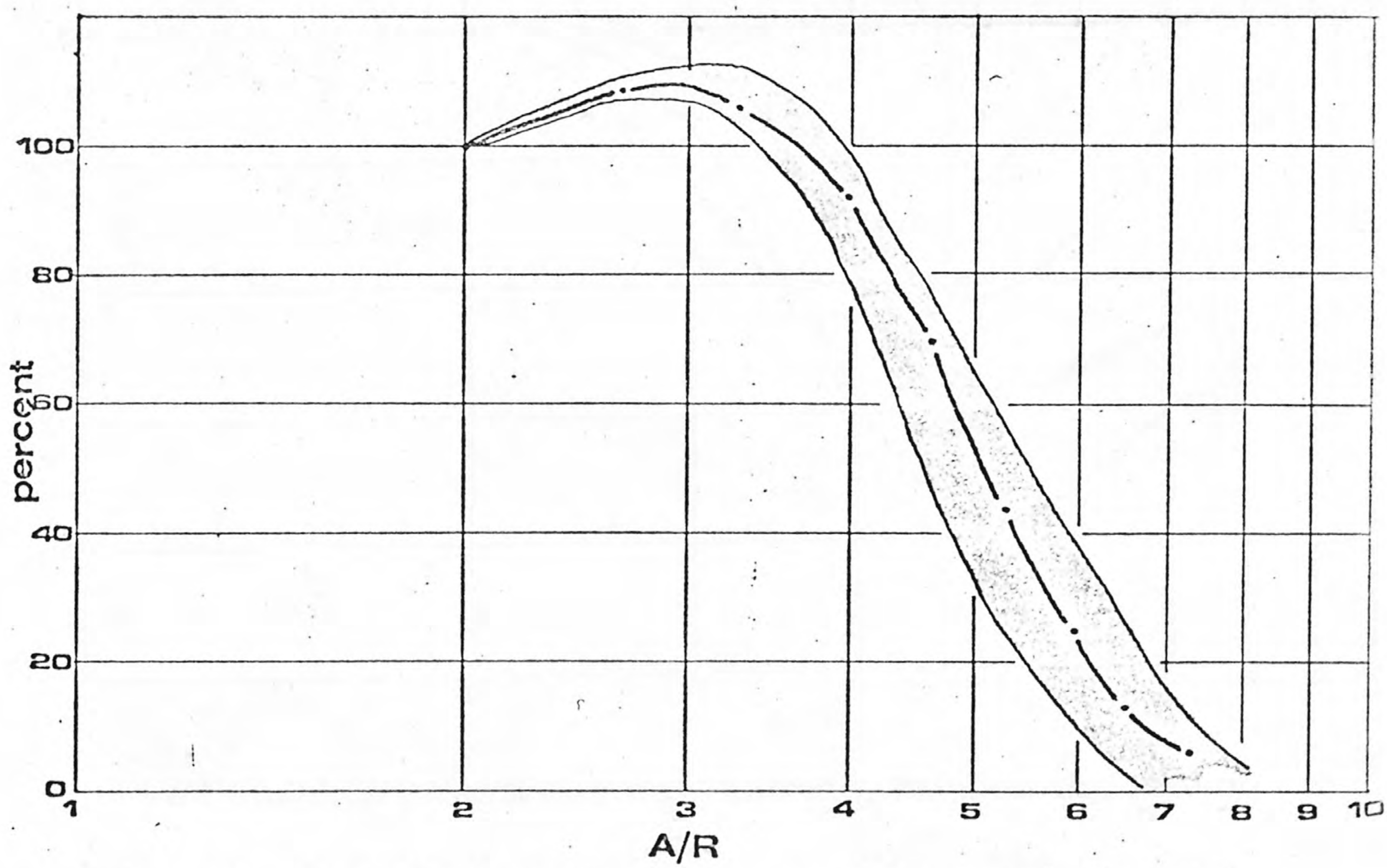

Figure 3. Real field response curve, Kilauea Iki, Hawaii.

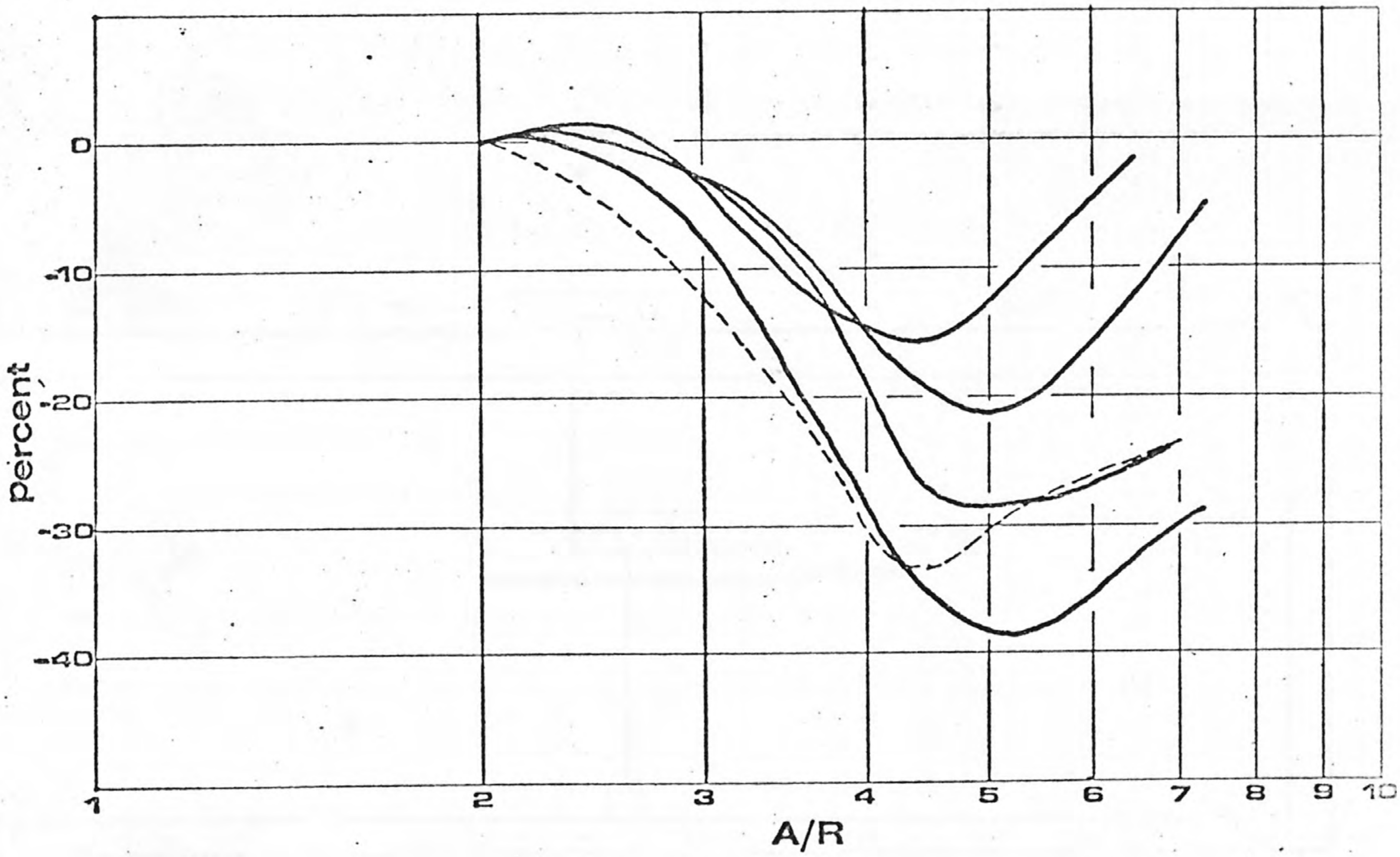

figure 4. Imaginary response field curves, Kilauea Iki, Hawaii

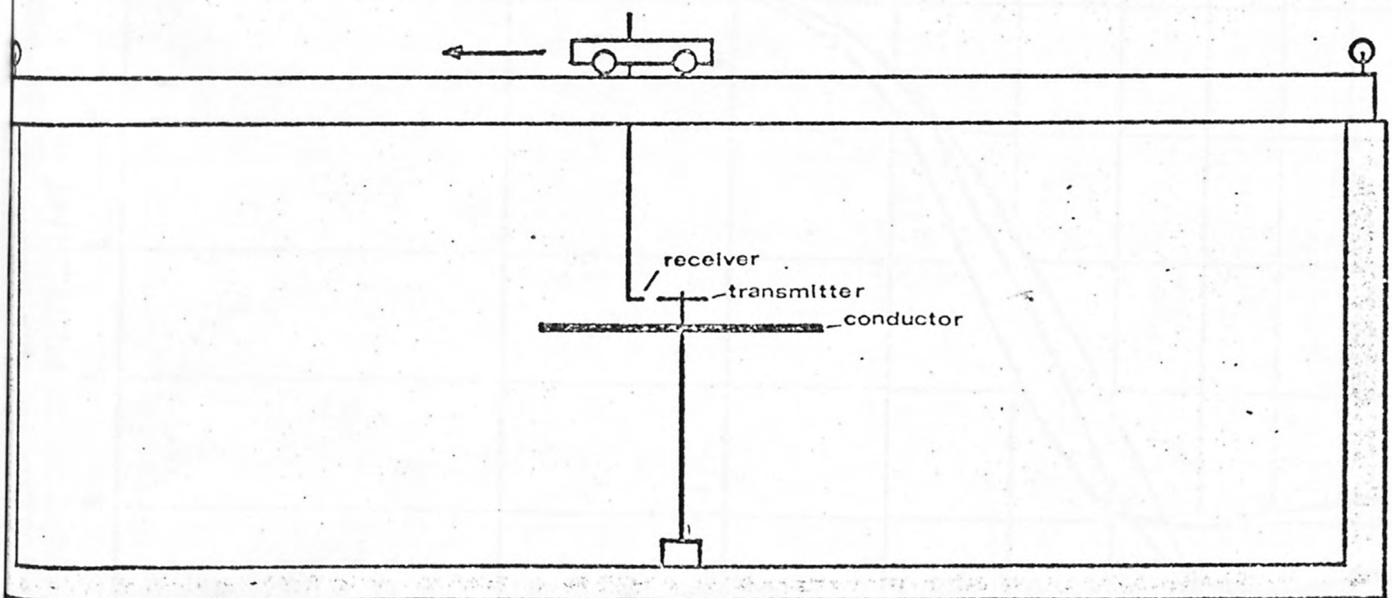

Figure 5. SCHEMATIC OF MODEL TANK SETUP

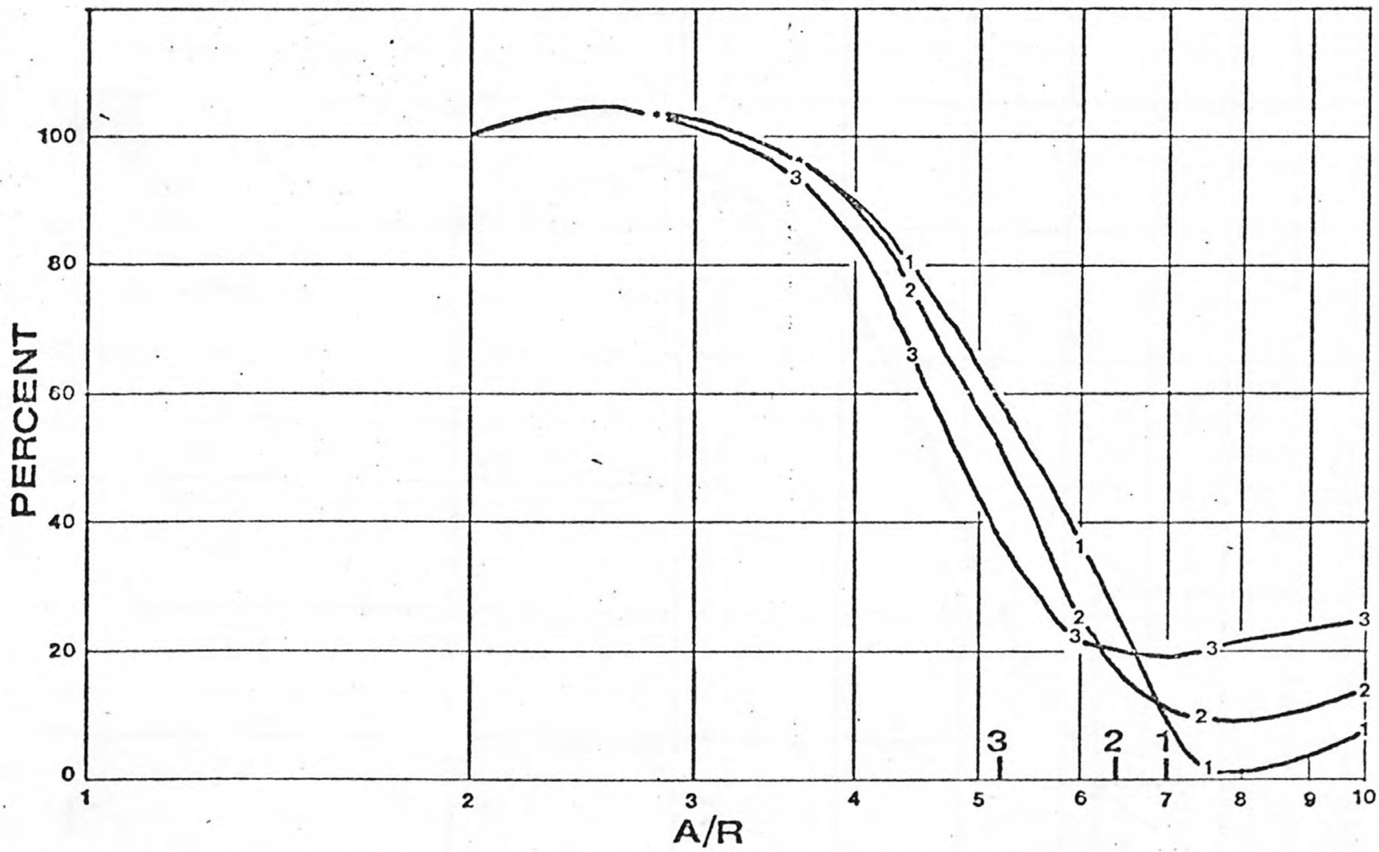

Figure 6. MODEL CURVES REAL COMPONENT

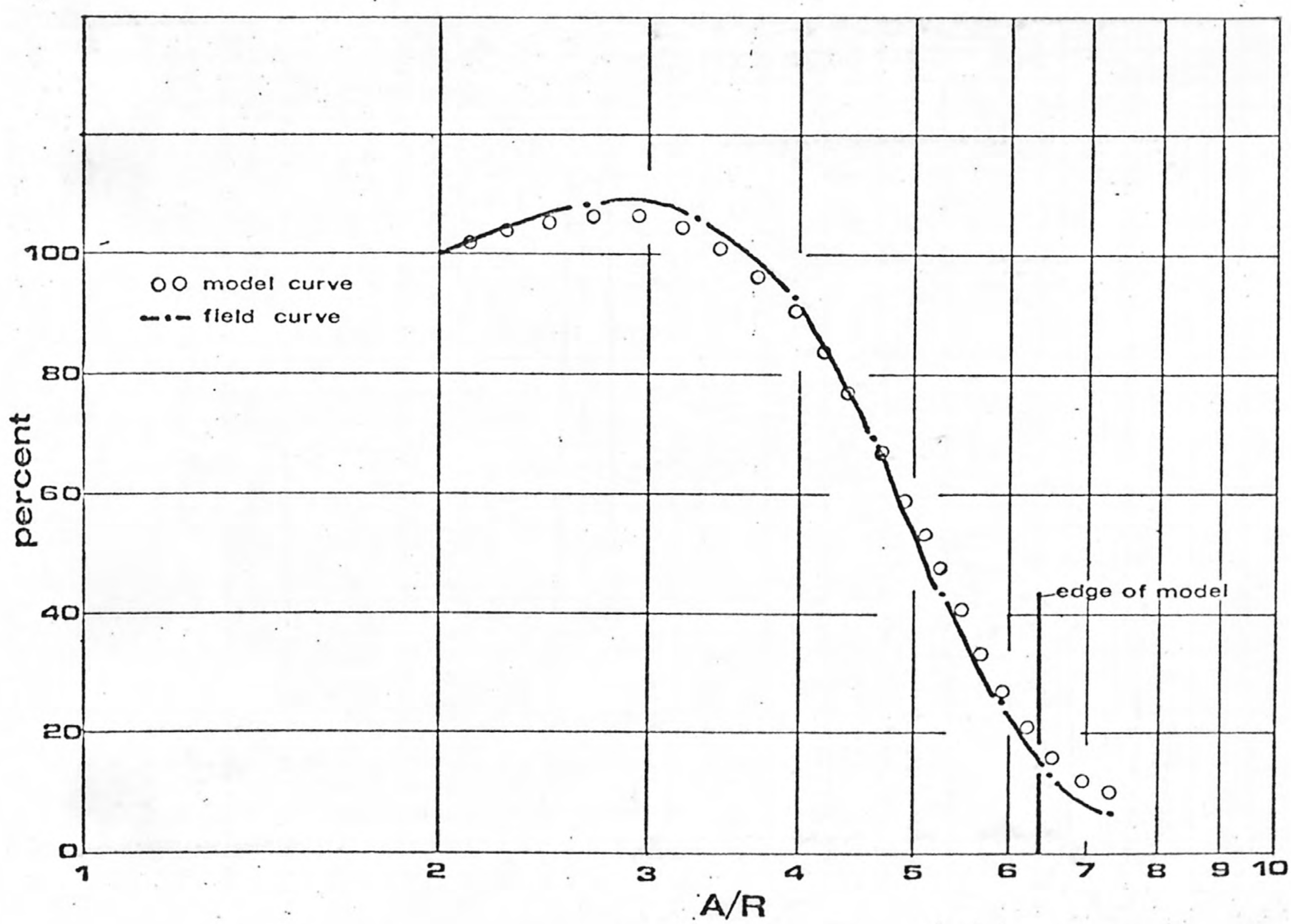

Figure 7. Model-field curve fit.

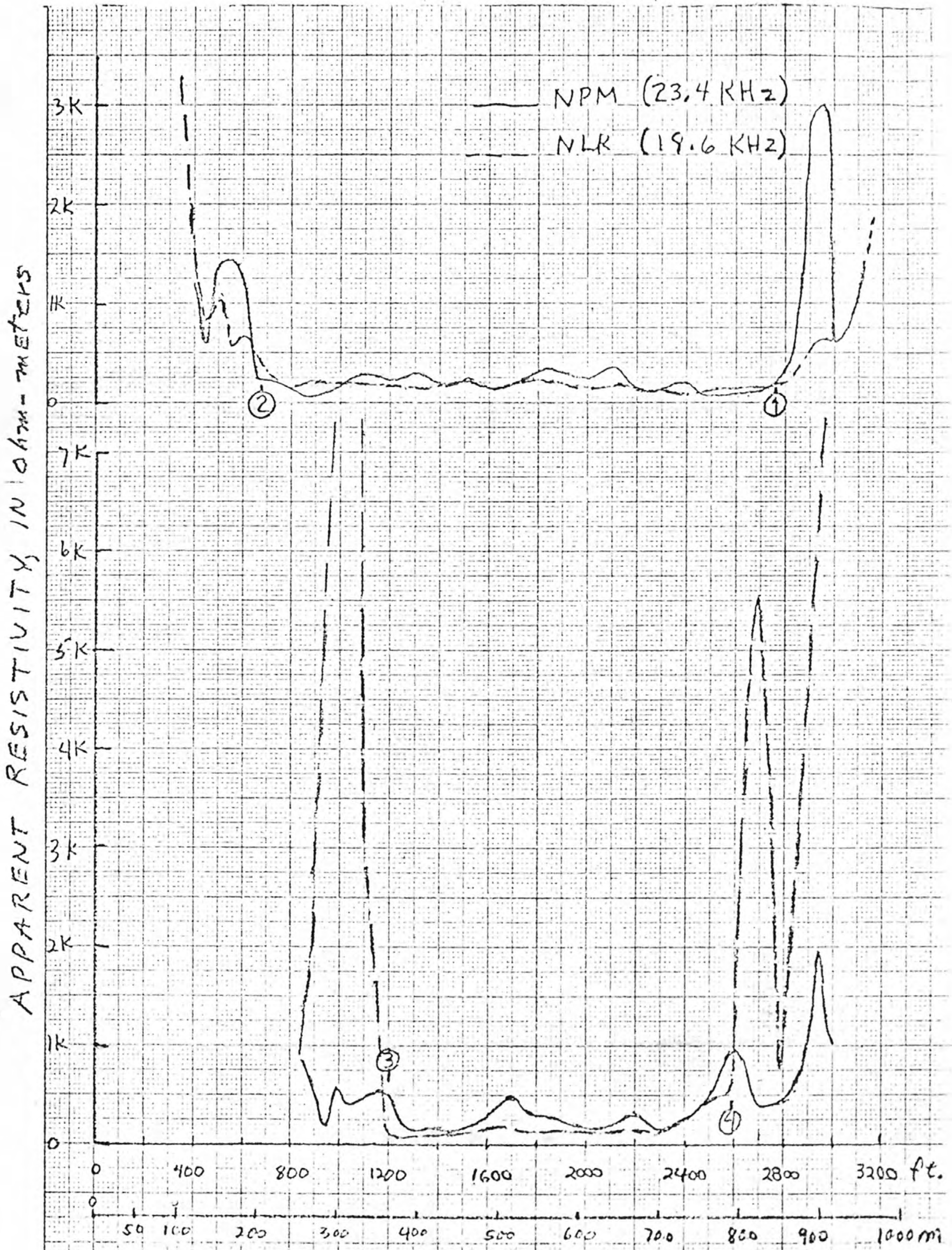
NPM (23.4 KHz)
NLK (19.6 KHz)
APPARENT RESISTIVITY IN ohm-meters
3K
2K
1K
0
7K
6K
5K
4K
3K
2K
1K
0
0
400
800
1200
1600
2000
2400
2800
3200 ft.
0
50
100
200
300
400
500
600
700
800
900
1000 m
1
2
3
4

Figure 8

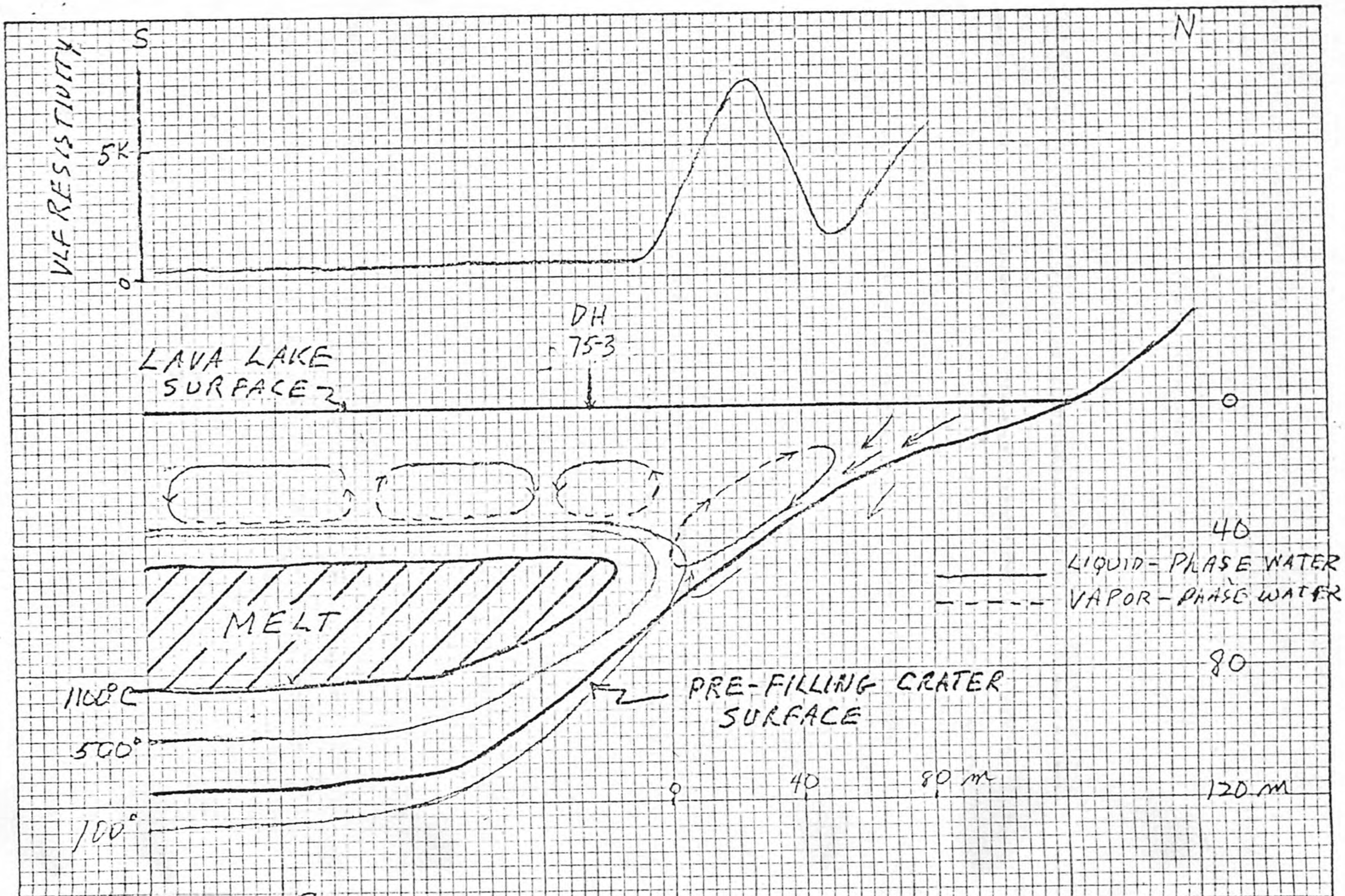
S
N
VLF RESISTIVITY
5K
0
DH
75-3
LAVA LAKE
SURFACE
0
40
LIQUID-PHASE WATER
VAPOR-PHASE WATER
MELT
80
1100°C
PRE-FILLING CRATER
SURFACE
500°
0
40
80 m
120 m
100°

Figure 9